



ELSEVIER

Available online at [www.sciencedirect.com](http://www.sciencedirect.com)

SCIENCE @ DIRECT®

Astroparticle Physics 20 (2004) 405–412

Astroparticle  
Physics

[www.elsevier.com/locate/astropart](http://www.elsevier.com/locate/astropart)

# Signatures of ultra-high energy cosmic ray composition from propagation of nuclei in intergalactic photon fields

T. Yamamoto <sup>a,\*</sup>, K. Mase <sup>b</sup>, M. Takeda <sup>c</sup>, N. Sakaki <sup>c</sup>, M. Teshima <sup>d</sup>

<sup>a</sup> *Center for Cosmological Physics, University of Chicago, 933 East 56th Street, Chicago, IL 60637, USA*

<sup>b</sup> *Institute for Cosmic Ray Research, University of Tokyo, Chiba 277-8582, Japan*

<sup>c</sup> *RIKEN (The Institute of Physical and Chemical Research), Saitama 351-0198, Japan*

<sup>d</sup> *Max-Planck-Institute für Physik, Föhringer Ring 6, 80805 München, Germany*

Received 11 April 2003; received in revised form 9 August 2003; accepted 10 August 2003

## Abstract

We present a calculation of nuclei propagation with energies above  $10^{18}$  eV in the intergalactic photon field. The calculation is based on a Monte-Carlo approach for the nucleus–photon interaction as well as the intergalactic magnetic field. We then assume that the ultra-high energy cosmic rays (UHECR) are nuclei which are emitted from extra-galactic point sources. Four bumps are found in the energy spectrum of the UHECR which form clusters in the distribution of their arrival directions. Based on this calculation, the energy distribution of the clustered events is discussed.

© 2003 Elsevier B.V. All rights reserved.

*Keywords:* Ultra-high energy cosmic rays; Propagation

## 1. Introduction

After a few decades of observation by several projects, the nature of the UHECR is gradually being revealed. Based on the observational results, there is no doubt of the existence of UHECR up to  $10^{20}$  eV [1–3]. This has led to consideration of a large number of production models. Most of the models assume that UHECRs are protons or photons.

Several studies of anisotropy have been done to reveal the origin of the UHECR [4–9]. Around  $10^{18}$  eV, a large scale anisotropy which is correlated to the Galactic center was reported by AGASA group [4]. This result, if confirmed, supports an interpretation that cosmic rays below  $10^{18}$  eV are dominated by a Galactic origin. Above this energy, however, no significant large scale anisotropy has been detected by AGASA [6].

On the other hand, AGASA reported clusters in the distribution of arrival directions including four doublets and two triplets with energy above  $4 \times 10^{19}$  eV [5,6]. This results indicate that the UHECR come from extra-galactic point sources. The cluster events reported by AGASA are composed of particles with different energies. A possible explanation would be neutral particles (like

\* Corresponding author. Tel.: +1-7738349958; fax: +1-7738348279.

*E-mail address:* [tokonatu@icrr.u-tokyo.ac.jp](mailto:tokonatu@icrr.u-tokyo.ac.jp) (T. Yamamoto).

neutrinos) propagating in straight lines from the source. Another possible explanation would be charged particles with large rigidity, i.e. with small charge like protons. If there is only the effect of the Galactic magnetic field then protons of different energy can arrive at same direction [10]. However, these two possibilities cannot explained the three bumps in the energy spectrum of the cluster events between  $10^{18.8}$  and  $10^{19.8}$  eV [13] reported by AGASA. This structure is not statistically significant. However, it suggests to us the interesting possibility that UHECR might be nuclei as it will be discussed in this paper. In this scenario, cluster events would be formed by particles with different charge and energy but with the same rigidity. The atomic number of the primary cosmic ray does not affect the energy determination of AGASA which measures the number of charged particles on the ground. However, the capability of AGASA to measure the composition of the primary cosmic rays is not very strong [11]. Nevertheless, the structure of the energy distribution of the cluster events may be used to measure of the composition indirectly as discussed in this paper.

If UHECR come from point sources and their rigidity is large enough or their source close enough so the direction is not lost, a fraction of the particles emitted by the source will arrive within a small angle from the source position. These particles are what we will call in this paper “small deflection angle” particles. Clusters will be formed when the number of particles expected within this angle in our experiment is larger than one. The small deflection angle particles should represent the cluster events observed by AGASA.

UHE protons should interact with cosmic microwave background radiation (CMBR) and lose energy by photo-pion production. For this reason,  $10^{20}$  eV protons cannot propagate in intergalactic space beyond 50 Mpc, leading to a cut-off in the spectrum below  $10^{20}$  eV, the so called GZK cut-off. On the other hand heavy nuclei will interact during its propagation with the Intergalactic Infrared Background Radiation(IIBR). Unfortunately the IIBR cannot be measured directly so far because of the strong background of infrared photons of Galactic origin. The main component of the IIBR is thought to be red-shifted stellar emission and

reemission from interstellar dust. The UHE nucleus should be disintegrated by the IIBR and lose energy by the photo-disintegration interaction. For this reason, it was believed that the attenuation length of UHE nuclei is shorter than that of protons in intergalactic space [14,15]. However, recent calculations which are based on empirical data show the IIBR density is much lower than originally thought [16]. The lack of absorption in the energy spectrum of very high energy gamma rays from AGNs strongly supports this calculation. Using this result, the attenuation length of the UHE nuclei in the intergalactic photon field was re-estimated [17] and found to be longer than that of a proton (a few 100 Mpc for  $10^{20}$  eV Fe).

We simulate the propagation of UHE nuclei which are emitted from extra-galactic point sources based on a Monte-Carlo approach. Using this simulation, we found structures in the energy distribution of the UHE nuclei which are observed as cluster events on the earth. In Section 2 we briefly describe the interaction of nuclei with background photons. In Section 3 we describe the scattering of the nuclei by the intergalactic magnetic field. In Section 4 we show the result of this simulation. We conclude in Section 5 and discuss the results briefly.

## 2. Interaction of nuclei with background photons

There are three processes which affect cosmic rays during intergalactic propagation: energy loss by interaction with cosmic background radiation; deflection by magnetic fields; and energy loss by adiabatic expansion of the universe. The effect of the adiabatic expansion is negligibly small if propagation distances are less than 1 Gpc.

There are four interaction processes of cosmic rays with intergalactic background radiation. The first process, Compton interaction, is negligibly small for our purpose. The second process is pair-production of  $e^+e^-$ . This interaction can occur if the energy of the background photon is greater than 1 MeV in the rest system of the nucleus. If the Lorentz factor of the nucleus is larger than  $10^9$ , it will efficiently interact with the CMBR (Fig. 1). In this case, the energy loss rate ( $dE/dt$ ) is propor-

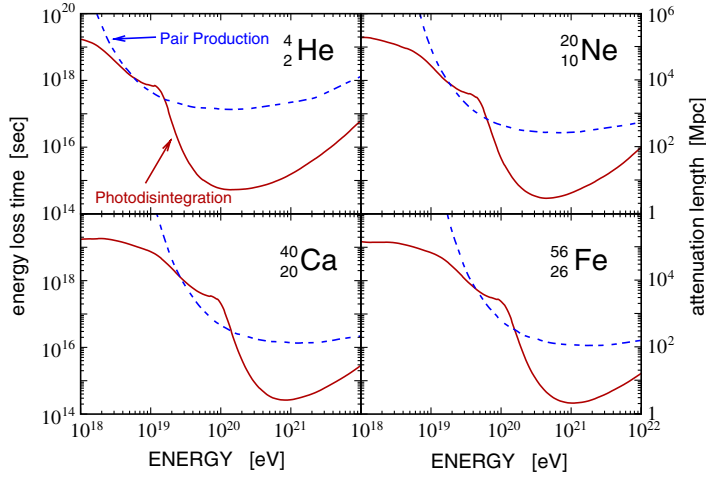


Fig. 1. Energy loss time of different mass nuclei as a function of energy. Solid line is that of single-nucleon emission by photo-disintegration and dashed line is pair production [17].

tional to the square of the charge of the nucleus. The third process is photo-production which mainly affects protons with energy greater than  $10^{20}$  eV. The interaction of heavier nuclei with the CMBR by this process is negligible for the energy range considered in this paper.

The fourth process is photo-disintegration. The nucleus interacts with the background photon and disintegrates to a lighter nucleus. In this paper, we calculate this process by a Monte-Carlo method according to [15,17]. These authors parametrized the total cross-section  $\sigma(\epsilon)$  as a function of photon energy in the rest frame of the nucleus. Then the probability of photo-disintegration per unit length  $R$  is calculated by following equation:

$$R = \int_0^\infty n(\epsilon) \left[ \frac{\int_0^{2\gamma\epsilon} \sigma(\epsilon') \frac{\epsilon'}{\epsilon} d\epsilon'}{2\gamma\epsilon} \right] d\epsilon \quad (1)$$

where  $\epsilon$  and  $\epsilon'$  are the energies of the photon in the lab frame and in the nucleus rest frame respectively,  $n(\epsilon)$  is the differential number density of photons including the CMBR and the IIBR [17], and  $\gamma = \epsilon'/\epsilon$  is the Lorentz factor of the nucleus. The term inside the bracket corresponds to the angle-averaged cross-section for a photon of energy  $\epsilon$ . Fig. 1 shows characteristic time  $\tau$  for the energy loss due to photo-disintegration for a

single-nucleon emission process as a function of energy.  $\tau$  is defined by following equation:

$$\frac{1}{\tau} = \frac{1}{E} \frac{dE}{dt} \quad (2)$$

The effect of the CMBR is maximized when the Lorentz factor  $\gamma$  is around  $10^{10}$ . In case of Fe, this value corresponds to an energy of  $10^{21}$  eV, yielding a value of  $\tau = 2 \times 10^{14}$  s (2 Mpc). Because the IIBR density is much lower than the CMBR density,  $\tau$  increases rapidly at lower energy.  $\tau$  of Fe with  $10^{20}$  eV is about  $2.5 \times 10^{17}$  s (2.5 Gpc). In general, one or a few nucleons and a single lighter nucleus are emitted by this interaction. The Lorentz factor is conserved at each photo-disintegration interaction, though it is reduced by the pair-production. Finally, UHE particles will pile up at a Lorentz factor around  $10^9$ . When  ${}^9\text{Be}$  is disintegrated, one proton and two He are emitted. Therefore no nucleus is created with a mass number between 5 and 8.

The interaction probability is calculated for every possible photo-disintegration process involving the emission of one or more nucleons for all nuclei lighter than Fe. Based on these probabilities, the propagation of the nucleus is simulated by the Monte-Carlo method. The effects of pair production, the adiabatic expansion, and photo-pion

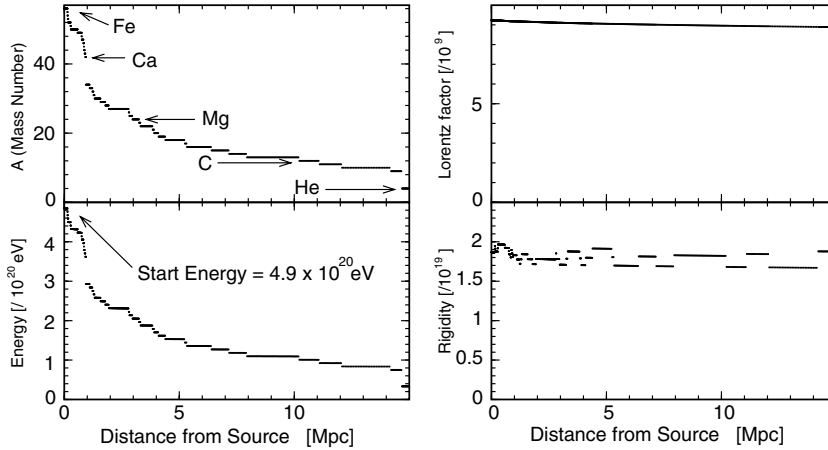


Fig. 2. Life of an Fe nucleus. An Fe is emitted with an energy of  $4.9 \times 10^{20}$  eV. The Fe is disintegrated during its propagation and turn into lighter nucleus with the emission of nucleons. These figures show the properties of the surviving nucleus as a function of propagation distance from the source. The upper and lower left panels show the variation of the mass number and the energy of the surviving nucleus respectively. These parameters change in a similar way. The upper and lower right panels show the variation of the Lorentz factor and the rigidity respectively. In comparison with the energy, the Lorentz factor changes smoothly because the photo-disintegration process does not change the Lorentz factor. Only the pair-production process affects this parameter. Therefore variations of the Lorentz factor and the rigidity are smaller than that of the energy. The fluctuation of the rigidity in lower right panel is caused by the variation of the ratio of mass number to charge ( $A/Z$ ).

production for protons are taken into account analytically in this simulation.

Fig. 2 shows the life of an Fe nucleus whose initial energy is  $4.9 \times 10^{20}$  eV. The Fe is disintegrated during its propagation and turns into a lighter nucleus with the emission of nucleons. When the nucleus is  $^{42}\text{Ca}$ , four protons and four neutrons are emitted. Then a sulfur is created. In comparison with energy, the Lorentz factor changes smoothly because photo-disintegration process does not change the Lorentz factor. This process makes a lighter nucleus and nucleons with same Lorentz factor.

### 3. Scattering by the intergalactic magnetic field

The effect of magnetic fields is described by the rigidity defined as the ratio of energy to charge ( $=E/Z$ ). Particles with small rigidity are deflected by the magnetic field and cannot be observed as a cluster. The deflection of magnetic field increases the propagation time, and therefore particles emitted from distant sources may not reach to the

observer. We calculate the effect of the intergalactic magnetic field based on a Monte-Carlo method.

To simulate the scattering by the intergalactic magnetic field, we assume a Kolmogorov spectrum for the random magnetic field according to the reference of [18]. In this reference, authors divide space in a lattice of 250 kpc cubes. The lattice is filled with a random magnetic field which follows the Kolmogorov spectrum with three logarithmic scales. Three field vectors of random orientation are sampled at scales  $l = 1000, 500,$  and  $250$  kpc with amplitudes proportional to  $l^{1/3}$ . The final magnetic field in each 250 kpc cube is vectorial sum of these three vectors. The average magnitude of the magnetic field is assumed to be 1 nG. Particles propagate in spiral trajectories until they leave the lattice. Fig. 3 shows examples of the trajectories. Fe with energy of  $10^{18}$  eV does not rapidly lose energy by the interaction with photons, and is trapped by the magnetic field inside 1 Mpc cubes. In case of  $2 \times 10^{20}$  eV, Fe is disintegrated by the photons rapidly and the products propagates close to a straight line in the initial direction of the Fe.

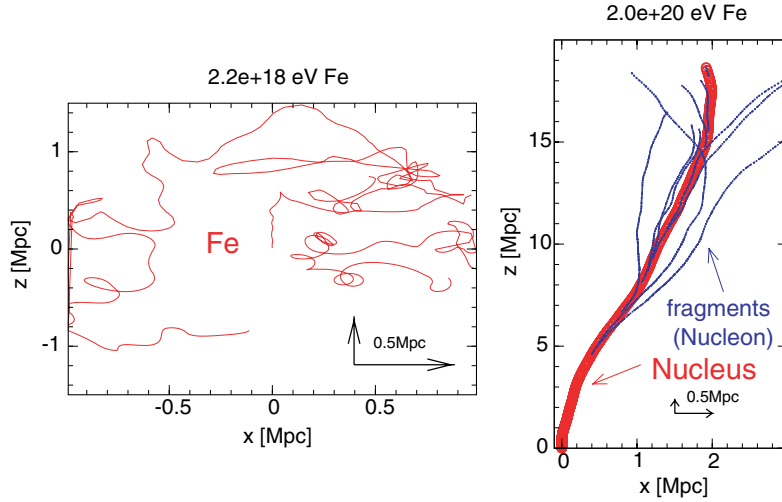


Fig. 3. Examples of trajectory of UHE Fe in the intergalactic magnetic field. A Fe emitted in the  $z$  direction with an energy of  $2 \times 10^{18}$  eV from a source located on the origin in left panel. A projection of the trajectory on  $x$ - $z$  plane is shown. At this energy, the attenuation length is sufficiently large. Therefore the energy of the particle is almost conserved and the particle is scattered by the magnetic field significantly. The Fe cannot propagate a distance of more than 1 Mpc from the source. In the right panel, a Fe with energy of  $2 \times 10^{20}$  eV emitted in the same direction as the left panel. The Fe and secondary nuclei are indicated by the wide line and secondary nucleons (proton and neutron) are indicated by the narrow lines. The Fe interact with photons rapidly and is disintegrated to lighter nuclei with emission of protons and neutrons. All of the particles are scattered by the magnetic field but deflection angle is comparatively small. Arrows in the panels indicate 0.5 Mpc distance.

#### 4. Energy distribution

In our simulation, the source energy spectrum  $dN(E)/dE$  is assumed to have a power law dependence  $E^{-2}$  and have a cut-off at the energy of  $Z \times 2 \times 10^{19}$  eV, where  $Z$  is charge of each primary nucleus. Below 300 MeV/nucleon, the cosmic nuclear composition can be divided to four types: He, CNO, Ne–Si, and Fe. Nuclear abundance between He and C is relatively low as well as between Si and Fe. We treat the composition as four components,  ${}^4_2\text{He}$ ,  ${}^{14}_7\text{N}$ ,  ${}^{24}_{12}\text{Mg}$ , and  ${}^{56}_{26}\text{Fe}$ . The fraction of these nuclear abundances in the UHE region are unknown. Therefore we assume equal fractions relative to He at the source. 20 000 particles are created for each nucleus.

Fig. 4 shows the variation of the energy distribution after propagation from a single source initiated by Fe through the photon and magnetic field. Nuclei with Lorentz factor above  $10^9$  interact with the CMBR rapidly. After 1 Mpc propagation a small pile-up is induced below the corresponding energy and the maximum energy of the particle is

reduced. Since we assume a cut-off energy in the source spectrum, protons are emitted with energies below  $Z/A \times 2 \times 10^{19}$  ( $\simeq 10^{19}$ ) eV where  $A$  is mass number of the primary nucleus. The number of low energy nuclei ( $< 10^{19}$  eV) increases up to 10 Mpc from the source since these nuclei are trapped by the magnetic field. These low energy nuclei cannot propagate farther than few 10 Mpc. Therefore, the energy distribution becomes steeper for distances below 10 Mpc and flatter for larger distances. No particles remain after propagation of a few 100 Mpc.

Fig. 5 is same result as lower left panel of Fig. 4. The energy distributions at a distance of 50 Mpc from the source are shown for different deflection angle (angle between the arrival direction and the source position). Particles with the deflection angle smaller than  $2.5^\circ$ ,  $5^\circ$ ,  $10^\circ$ ,  $180^\circ$  are counted ( $180^\circ$  corresponds to the entire sample of particles included in Fig. 4). Three bumps appear clearly in the distribution of particles with a small deflection angle. The bump below  $10^{19}$  eV is composed of protons which are emitted from higher energy nuclei in the vicinity of the observer who is located

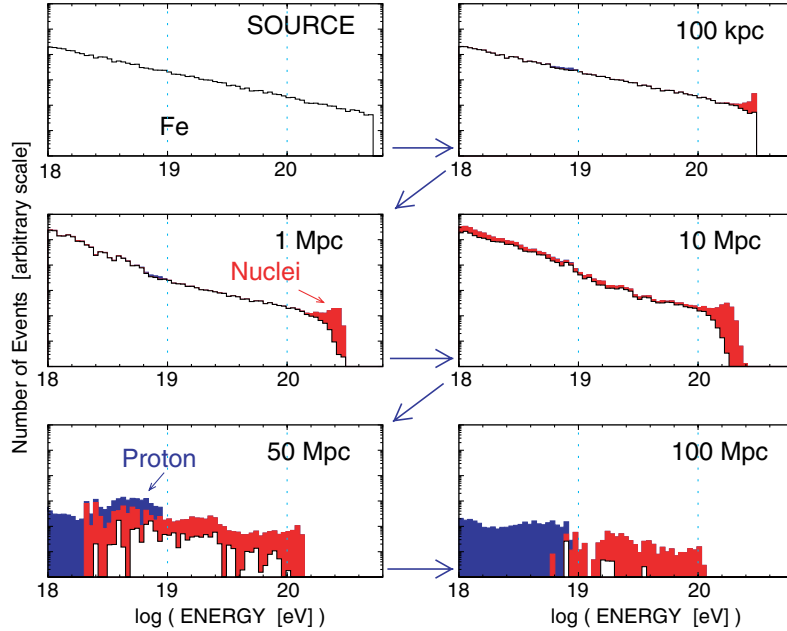


Fig. 4. Variation of energy distribution of particles that began as Fe after propagation over various distances from a single source. The distances from the source are indicated in each panel. The number of particles (arbitrary scale) are shown as a function of energy. Primary nuclei (Fe), secondary lighter nuclei, and protons are indicated by white, light shade and dark shade in the histograms respectively. The differential source spectrum is assumed to be a power law,  $\propto E^{-2}$ , with energy cut-off at  $Z \times 2 \times 10^{19}$  eV (upper left panel). At 100 Mpc from the source, most of the Fe disappears because of their low rigidity.

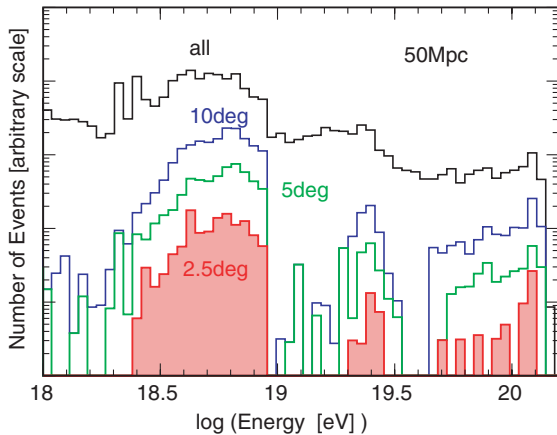


Fig. 5. Energy distribution of the particles at the 50 Mpc distance from a source as a function of deflection angle by the magnetic field. The assumed source spectrum is same as in the previous figure. The number of particles with the deflection angle smaller than 2.5°, 5°, 10°, 180° (same as previous figure) are shown.

at 50 Mpc distance from the source. The bump around  $10^{19.4}$  eV is composed of He, and the bump

above  $10^{19.6}$  eV is composed of nuclei heavier than Be.

These bumps can be explained as follows: The rigidity is proportional to  $Z^{-1}$  and  $E$ , and  $Z$  is approximately proportional to its mass number  $A$  while the Lorentz factor is proportional to  $A^{-1}$  and  $E$ . This means that the Lorentz factor of a particle is approximately proportional to the rigidity. Therefore, if the Lorentz factor of the nucleus is large, the energy is reduced by the photo-disintegration. If the Lorentz factor is small, the particle is deflected by the magnetic field due to its small rigidity. However particles with Lorentz factor of about  $10^9$  remain after applying the deflection angle cut. As a result, the bumps appear in the energy distribution of the small deflection angle particles at positions dependent on the mass numbers. The combination of the photo-disintegration and the magnetic field acts as a “filter” for  $\gamma = 10^9$  particles. The energy distribution of the small deflection angle particles shows clearly the spectral features created by interactions with

the intergalactic photon background and magnetic fields during their propagation.

If the sources are distributed uniformly in the Universe, the expected energy distribution measured at the earth can be estimated by adding up linearly the energy distributions corresponding to different distances from the source. In Fig. 4 the number of particles around  $10^{20}$  eV coming from sources at 100 Mpc is 1.5 orders of magnitude smaller than from sources at 100 kpc. When adding linearly the different distances, the number of particles from sources at 100 Mpc is enhanced three orders of magnitude compared to sources at 100 kpc. Therefore, the contribution to the energy spectrum at earth is increasing with the distance to the source till a couple of hundred Mpc. On the other hand, most of the low energy particles emitted by distant sources will be trapped by the magnetic field and they will not reach the earth. However, the low energy secondaries resulting from the photo-disintegration of high energy heavy nuclei close to earth will regenerate the low energy spectrum coming from distant sources. Therefore, even at low energies we will still be dominated by the contribution of distant sources. The spectrum of small deflection angle particles will follow the same behavior, i.e. the contribution of sources at large distances to the spectrum exceed largely the one from small distant sources, even if the fraction of small deflected particles for closer sources is slightly larger.

It should be noted that the relation between cluster events and small deflection particles is qualitatively clear but difficult to estimate quantitatively. Current work is in progress for a better comparison with experimental data.

Fig. 6 shows the result of the expected energy distribution under the assumption that the sources are distributed uniformly in the Universe. The solid line shows the expected energy distribution of all the particles that reach the earth. The expected energy spectrum is steeper than the source spectrum. Above  $10^{20.2}$  eV, the energy spectrum becomes even steeper and the maximum energy is about  $10^{20.4}$  eV. The exact details of the upper end of the spectrum will depend on the source spectrum cut-off.

The dashed lines in Fig. 6 show the expected energy distribution of the small deflection angle

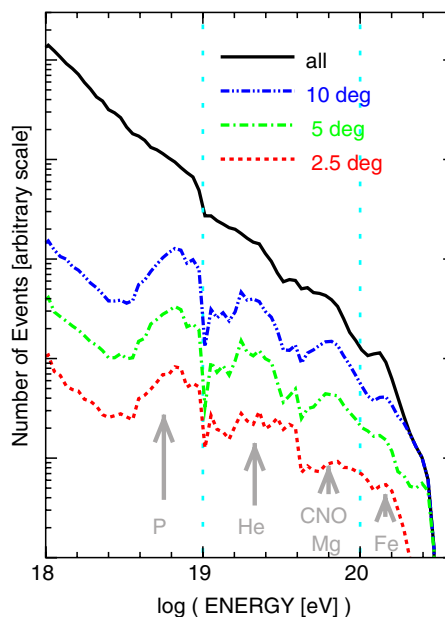


Fig. 6. The expected energy distribution of particles after propagation under the assumption that point sources are distributed uniformly in the universe. The solid line shows the energy distribution with no deflection angle cut. The other (dashed dots) lines show the energy distributions of the particle with deflection angles smaller than  $10^\circ$ ,  $5^\circ$ , and  $2.5^\circ$ . Particles with lower rigidity are scattered by the magnetic field. Larger rigidity particle are disintegrated by the photon field due to their large Lorentz factor.

particles. This spectrum is much flatter than the source spectrum. Four bumps appear in this figure. The bump just below  $10^{19}$  eV corresponds to protons and strongly depends on the cut-off energy at the source. The bump around  $10^{19.3}$  eV is composed of deuteron and He. Every nucleus with a Lorentz factor around  $10^9$  contributes to the He bump after propagation. The bump between  $10^{19.6}$  and  $10^{20}$  eV correspond to nuclei with mass between Be and Mg. The bump above  $10^{20.1}$  eV is composed of Fe and other nuclei of similar atomic number.

This total spectral structure bears a striking resemblance to the result of AGASA [1,12,13].

## 5. Results and discussion

We have simulated propagation of UHE nuclei which are emitted from extra-galactic point

sources using a Monte-Carlo approach. Using this simulation, structures in the energy distribution of the small deflection angle particles have been predicted. In this simulation, we assume that UHECR are nuclei which are emitted from extra-galactic point sources. The nuclei interact with cosmic background radiation and lose energy during their propagation. Based on recent estimations of the IIBR, it has been shown that UHE nucleus can propagate longer distances than a proton with same energy. It is also expected that heavier nuclei are accelerated more efficiently to high energy than lighter nuclei or protons.

We have considered the effect of the intergalactic magnetic fields. We use a Kolmogorov spectrum for random magnetic fields that is 1 nG in average intensity with a 1 Mpc correlation length. The energy distribution of the particles with deflection angles smaller than  $10^\circ$ ,  $5^\circ$ , and  $2.5^\circ$  are investigated. Consequently, for this model no cosmic rays can be observed after propagation of a few hundred Mpc. Lower rigidity particles are deflected by the magnetic field relatively rapidly. Particles with larger Lorentz factor lose energy by photo-disintegration. Since the rigidity and the Lorentz factor are proportional to the particle energy and inversely proportional to the mass number, particles which have common a Lorentz factor, or similar rigidity, remain after the deflection angle cut. The Be–Mg bump appears at an energy more than four times larger than the He bump, and the Fe bump appear around six times larger energy. The rigidity gives a lower bound and energy loss gives an upper bound on the bumps. The energy distribution of the clustered events observed by AGASA can be explained by this model.

In the simulation, we assume a specific intergalactic magnetic field distribution, cut-off energy and source composition of primary nuclei. The Galactic magnetic field is ignored in this simulation. The events with certain deflection angle are selected and shows the effects due to the intergalactic photons and magnetic fields. This effect depends on the strength and correlation of the

intergalactic magnetic field. This dependence gives an ambiguity to the analysis since the deflection angle cut is adjustable. Therefore, this angle should be treated carefully.

This result suggests that if we detect few hundred events above  $10^{20}$  eV in future experiments, we should be able to extract the structure of the bumps in the energy distribution of cluster events. The Pierre Auger Observatory is quite sufficient for this purpose and may confirm the signature of nuclei in the spectrum in the near future.

### Acknowledgements

We thank Angela Olinto, Alan Watson, James W. Cronin, Maximo Ave, Aaron Chou, and Medina Tanco for useful discussions. This research was supported by grant NSF PHY-0114422 to the Center for Cosmological Physics, University of Chicago, and grant NSF PHY0103717.

### References

- [1] M. Takeda et al., *Phys. Rev. Lett.* 81 (1998) 1163.
- [2] E.J. Bird et al., *Astrophys. J.* 351 (1994) 491.
- [3] T. Abu-Zayyad et al., astro-ph/0208301.
- [4] N. Hayashida et al., *Astropart. Phys.* 10 (1999) 303.
- [5] Y. Uchihori et al., *Astropart. Phys.* 13 (2000) 151.
- [6] M. Takeda et al., *Astrophys. J.* 522 (1999) 225.
- [7] G.R. Farrar, P.L. Biermann, *Phys. Rev. Lett.* 81 (1998) 3579.
- [8] G.R. Farrar, P.L. Biermann, *Phys. Rev. Lett.* 83 (1999) 1999.
- [9] P.G. Tinyakov, I.I. Tkachev, *Phys. Rev. Lett.* 85, 1154.
- [10] J.W. Cronin, in: *Proceedings of EHECR Astrophysics and Future Observations*, Tokyo, Japan, September 1996.
- [11] K. Sinozaki et al., *Astrophys. J.* 571 (2002) 117.
- [12] M. Takeda et al., *J. Phys. Soc. Jpn. Suppl. B* 70 (2001) 15.
- [13] M. Takeda et al., in: *Proceedings of 27th ICRC 2001*, p. 341.
- [14] F.W. Stecker, *Phys. Rev.* 21 (1968) 1016.
- [15] J.L. Puget, F.W. Stecker, *Astrophys. J.* 205 (1976) 638.
- [16] M.A. Malkan, F.W. Stecker, *Astrophys. J.* 496 (1998) 13.
- [17] F.W. Stecker, M.H. Salamon, *Astrophys. J.* 512 (1999) 521.
- [18] T. Stanev et al., *Phys. Rev. D* 62 (2000) 093005.